AGU PUBLICATIONS

Space Weather

RESEARCH ARTICLE
10.1002/2016SW001491

Key Points:
- Under the scenarios explored potential daily lost GDP ranges from $6.2 to 42 billion for the U.S.
- The direct economic cost incurred within the blackout zone only represents approximately 49% of the total potential macroeconomic cost
- Cost-benefit analysis of investment in space weather forecasting and mitigation must take account of indirect supply chain loss

Supporting Information:
- Supporting Information S1

Correspondence to:
E. J. Oughton,
e.oughton@jbs.cam.ac.uk

Citation:
Oughton, E. J., A. Skelton, R. B. Horne, A. W. P. Thomson, and C. T. Gaunt (2017), Quantifying the daily economic impact of extreme space weather due to failure in electricity transmission infrastructure, *Space Weather*, *15*, 65–83, doi:10.1002/2016SW001491.

Received 5 AUG 2016
Accepted 3 DEC 2016
Published online 17 JAN 2017

Quantifying the daily economic impact of extreme space weather due to failure in electricity transmission infrastructure

Edward J. Oughton[1], Andrew Skelton[1], Richard B. Horne[2], Alan W. P. Thomson[3], and Charles T. Gaunt[4]

[1]Centre for Risk Studies, Judge Business School, University of Cambridge, Cambridge, UK, [2]British Antarctic Survey, Natural Environment Research Council, Cambridge, UK, [3]British Geological Survey, Natural Environment Research Council, Edinburgh, UK, [4]Department of Electrical Engineering, University of Cape Town, Cape Town, South Africa

Abstract Extreme space weather due to coronal mass ejections has the potential to cause considerable disruption to the global economy by damaging the transformers required to operate electricity transmission infrastructure. However, expert opinion is split between the potential outcome being one of a temporary regional blackout and of a more prolonged event. The temporary blackout scenario proposed by some is expected to last the length of the disturbance, with normal operations resuming after a couple of days. On the other hand, others have predicted widespread equipment damage with blackout scenarios lasting months. In this paper we explore the potential costs associated with failure in the electricity transmission infrastructure in the U.S. due to extreme space weather, focusing on *daily economic loss*. This provides insight into the direct and indirect economic consequences of how an extreme space weather event may affect domestic production, as well as other nations, via supply chain linkages. By exploring the sensitivity of the blackout zone, we show that on average the direct economic cost incurred from disruption to electricity represents only 49% of the total potential macroeconomic cost. Therefore, if indirect supply chain costs are not considered when undertaking cost-benefit analysis of space weather forecasting and mitigation investment, the total potential macroeconomic cost is not correctly represented. The paper contributes to our understanding of the economic impact of space weather, as well as making a number of key methodological contributions relevant for future work. Further economic impact assessment of this threat must consider multiday, multiregional events.

1. Introduction

Space weather disturbances of the upper atmosphere and near-Earth space can disrupt a wide range of technological systems [*Hapgood et al.*, 2012]. Over the past decade many reports have analyzed the potential effects of extreme space weather on electricity transmission infrastructure [*Space Studies Board*, 2008; *OECD*, 2011; *JASON*, 2011; *North American Electric Reliability Corporation*, 2012; *Cannon et al.*, 2013]. The economic costs associated with these extreme events have been heralded as being as high as $1–2 trillion in the first year, equivalent to a so-called "global Hurricane Katrina." To date, however, there has been a lack of *transparent* research around how these direct and indirect economic costs actually stack up, which is surprising given the level of debate and uncertainty surrounding the vulnerability of electricity transmission infrastructure to extreme space weather.

Research in this paper has been produced by a similar team that originally developed the Helios Solar Storm Scenario [*Oughton et al.*, 2016]—the first space weather stress test for the global insurance industry. Ultimately, these are different pieces of work. Helios purposefully explored the sensitivity of economic loss due to different temporal restoration periods, in order to provide a tool for stressing the portfolio exposure of global insurance companies. Helios is not a prediction but a hypothetical range of scenarios to enable mitigation of space weather risks in the insurance industry. On the other hand, this paper focuses purely on the daily direct and indirect economic consequences of how an extreme space weather event may affect U.S. domestic production, as well as other nations via supply chain linkages, based on different blackout zones.

Two opposing views have emerged. On the one hand, some believe that the potential damage would not be that large and that we are relatively well prepared to deal with an extreme geomagnetic disturbance (GMD). The worst case scenario is seen to be an electrical collapse of the transmission grid, probably initiated by loss

of voltage stability that will consequently protect the power system assets from damage. The grid connections could then be reestablished, leading to a disruption only lasting hours or a few days. On the other hand, there are those who believe that damage might be initiated before a system loses stability or might occur outside the region of the electrical collapse and that we could end up with extensive damage to equipment and a doomsday-type catastrophe scenario where blackouts last weeks, even months, until exposed assets (with many supply issues) are replaced. There is still disagreement among these perspectives, and therefore, it is not surprising that the recent U.S. National Space Weather Action Plan [*National Science and Technology Council*, 2015] identifies the need for improved assessment, modeling, and prediction of the impact of this threat on critical infrastructure systems. Although there has been substantial development in the credibility of these perspectives in recent years, there is a valid need to explore how disruption to electricity transmission infrastructure might affect our economy and society.

Modern economies increasingly rely on a variety of critical interdependent infrastructure systems powered by electricity. Although space weather can be caused by a variety of phenomena including solar particle events and bursts of electromagnetic radiation from solar flares, it is coronal mass ejections (CMEs) which are mostly associated with the long-term catastrophe scenarios that have been characterized in the literature. CMEs pose the main risk to Earth and its modern, technological society because large (10^{12} kg), relatively dense (100/cm^3), and fast ($>$500 km s^{-1}) CMEs hitting Earth with a southward interplanetary magnetic field direction (B_z) can give rise to extreme GMDs [*Möstl et al*., 2015; *Temmer and Nitta*, 2015; *Balan et al*., 2014]. Significant events may see quantities considerably larger than the numbers stated here. These have the potential to damage and disrupt the aviation, satellite, GPS, and electricity networks that our economy and society depend on. This is particularly problematic because failure in the power sector can cascade to other critical interdependent infrastructure systems, disrupting business activities and inducing a range of other economic and social consequences that can affect the global economy [*Ouyang*, 2014; *Anderson et al*., 2007; *Haimes and Jiang*, 2001; *Rinaldi et al*., 2001].

In particular, it is acknowledged that an extreme GMD has the potential to generate geomagnetically induced currents (GIC) that could initiate permanent damage to extra high voltage (EHV) transformers. Failure in these critical assets could cause system-wide instability issues leading to cascading failure. Further, such high-value assets are not necessarily easy to procure and replace in the short term. Understanding the economic impact of space weather risks can improve mitigation procedures and practices, as it can guide where limited resources should be allocated to improve economic resilience. Moreover, in industry it is not just utility companies who are concerned with catastrophe scenarios; the potential loss to insurance companies due to casualty and business interruption payouts could be enough to threaten the viability of certain companies in this sector (despite the use of limits and deductibles on insurance policies). Even during a relatively calm period of solar activity (2000–2010), *Schrijver et al*. [2014] have shown that there can be significant equipment loss and related business interruption claims for the insurance industry. Estimates of the potential economic loss associated with catastrophic events are able to be used to stress test asset exposure in the insurance industry and beyond. Indeed, in the UK General Insurance Stress Test 2015 undertaken by the Bank of England's Prudential Regulation Authority (PRA), insurers are required to undertake exposure stress tests for an extreme space weather event.

The scope of this paper has been guided by a recent workshop that focused on understanding the potential impacts of extreme space weather on the global economy. Held at the Judge Business School, University of Cambridge, UK, this event gathered together representatives from space physics, economics, catastrophe modeling, actuarial science, and law, with those from the property, casualty, and space insurance industry. Now that the motivation for the paper has been introduced, section 1 will present background material and examine past events. Section 2 will outline the methodology, and section 3 will report the results and discussion. Finally, conclusions will be presented in section 4.

1.1. Background

There are a wide variety of standardized magnetic indices recognized by the International Association for Geomagnetism and Aeronomy used to measure changes to Earth's magnetic field, which include *Dst*, *Kp*, *AE*, *AU*, *AL*, and *PC* [*ISGI*, 2016]. Though there is debate over the best method of measuring geomagnetic activity, the time rate of change (d*B*/d*t* in nanotesla per unit of time) of the geomagnetic field best represents the threat to EHV transformers and the electricity transmission network via GIC (when we refer to d*B*/d*t* in this

paper we specifically refer to the horizontal component, dH/dt, unless otherwise stated). The dB/dt induces a geoelectric field in the Earth that acts as a source for GIC and is dependent on ground conductivity. The dB/dt measure is relevant as it is the physical quantity that drives GIC in infrastructure by virtue of Faraday's law of electromagnetic induction and captures the rapid dynamic changes in electrical currents that usually flow in the ionosphere more than 90 km above ground in the auroral region above 50° geomagnetic latitude [e.g. *Thomson et al*., 2011]. However, low-latitude regions are more affected by the intensification of the higher-altitude ring current, as represented by the *Dst* index [*Sugiura*, 1963], a widely used characterization of geomagnetic activity [*Banerjee et al*., 2012].

The geomagnetic storm that affected Quebec in 1989, initiating the electrical collapse of the Hydro-Quebec power grid, is one of the best documented examples of a severe event during the space age, providing a useful starting point for exploring the impact of more extreme outcomes.

Severe and extreme space weather events occur often but do not always affect Earth. Many have reported on the powerful CME that erupted from the Sun on 23 July 2012 but missed Earth [*Intriligator et al*., 2015; *Temmer and Nitta*, 2015; *Liou et al*., 2014; *Baker et al*., 2013; *Ngwira et al*., 2013]. *Baker et al*. [2013] show that with an initial speed of 2500 ± 500 km/s, this event could be comparable with the largest events of the twentieth century ($Dst \sim -500$ nT), or even with the Carrington Event of 1859. However, with limited time series data it is challenging to estimate the size of the 1859 storm. There have been a number of ex post analyses of Carrington which estimate the size of the event to be $-850\,\text{nT} \leq Dst \leq -1760\,\text{nT}$ [*Tsurutani et al*., 2003; *Siscoe et al*., 2006; *Tsurutani et al*., 2012], roughly 1.5 to 3 times the size (at least in terms of *Dst*) of the 1989 geomagnetic storm in Quebec [*Boteler et al*., 1998; *Bolduc*, 2002]. With the July 2012 event being potentially comparable to Carrington in the most extreme scenario modeled ($Dst = -1182$ nT), *Baker et al*. [2013] therefore propose that this be used as the archetypal extreme space weather event for scenario-planning purposes. The July 2012 CME would therefore have caused an event that was roughly twice the size of the Quebec 1989 storm. In terms of relevant dB/dt estimates for geomagnetic activity, *Thomson et al*. [2011] estimate that we could see extreme values reaching 1000–4000 nT/min (one in 100 year event), or even 1000–6000 nT/min (one in 200 year event).

The proximity of a region to the auroral zone, and therefore the auroral electrojet currents flowing in the ionosphere, can increase the risk posed from this threat. Under extreme circumstances we know that this zone can move equatorward. For example, *Ngwira et al*. [2013] further confirm work by *Pulkkinen et al*. [2012], in that extreme activity tends to take place in a band between 50° and 55° geomagnetic latitude, with activity in this zone being a universal feature of extreme geomagnetic storms, reflecting findings elsewhere in the literature [*Thomson et al*., 2011]. In the Northern Hemisphere this geomagnetic latitude band includes many notable global cities including Chicago, Washington DC, New York, London, Paris, Frankfurt, and Moscow, while in the Southern Hemisphere it includes Melbourne and Christchurch. This shift in the auroral electrojet can cause unprepared regions not used to experiencing disruption from geomagnetic disturbances to be more at risk. In addition, areas with low deep-Earth conductivity are more at risk because higher GIC flows into the electricity network with the potential to cause serious damage to EHV assets. Having presented the background for this research, section 1.2 will now examine the characteristics of past events.

1.2. Past Events

When considering the impact of past space weather events, there are a number of well-documented recent examples. The 1989 storm which led to a widespread blackout in Quebec was caused by half-cycle saturation of power transformers and the induced harmonics tripping seven static reactive power compensators delivering reactive power [*Czech et al*., 1992; *Samuelsson*, 2013]. Massive reactive power shortage led to a voltage collapse of the Hydro-Quebec grid, with the total cost of equipment damage totaling $6.5 million. The net cost of the failure to Hydro-Quebec is estimated to be $13.2 million [*Bolduc*, 2002]. At the time of the incident, the power demand of the six million customers interrupted was approximately 14.5 GW, and, during the almost 9 h it took to restore supply, the demand would normally have increased to 19 GW. The geomagnetic scale of the event was estimated to be $Dst \sim -589$ nT, with dB/dt measurements in North America ranging from 300 to 600 nT/min. A later phase of the same storm also affected the U.S., including half-cycle saturation of a nuclear unit transformer which led to overheating and it being taken out of service at Salem, New Jersey [*NRC*, 1990]. In this case, only the output from the one power station was restricted and no blackout occurred.

During the 2003 "Halloween storm" (*Dst* ~ −353 nT) roughly 50,000 customers were left without power for an hour in Malmö, Sweden, when harmonic distortions produced by GIC tripped overly sensitive protective relays [*Pulkkinen et al*., 2005]. In this case, very high GIC of 330 A caused half-cycle saturation of a transformer, generating harmonics that caused protection to disconnect a 130 kV line [*Samuelsson*, 2013]. Since maintenance was taking place during the event and no backup was present, this led to the blackout. There were also reports of numerous transformers being badly affected with significant damage occurring in South Africa [*Gaunt and Coetzee*, 2007; *Ngwira et al*., 2011].

Increasingly, there is awareness that GIC risk is still present and a threat to low-latitude and midlatitude regions such as South Africa [*Gaunt and Coetzee*, 2007], Spain [*Torta et al*., 2012], Brazil [*Barbosa et al*., 2015; *Trivedi et al*., 2007], China [*Zhang et al*., 2015; *Liu et al*., 2008, 2009], Japan [*Watari et al*., 2009; *Watari*, 2015; *Fujii et al*., 2015], Australia and New Zealand [*Marshall et al*., 2011, 2013], and Turkey [*Kalafatoğlu et al*., 2015]. In light of the topic of this paper, this is particularly of concern if we were to see a significant auroral zone shift which could affect, for example, the southern states and midlatitude U.S.

The long restoration periods for damage to EHV transformers arise from the average lead time for a bespoke domestically manufactured transformer of 5 to 12 months and for internationally manufactured transformers of around 6 to 16 months [*Department of Energy*, 2014]. Moreover, there can be a protracted lead time before their manufacture and delays in physically installing them in place due to their size and weight, which require specialist transport and permits to move them along their chosen route.

The secondary effect of transformer damage, including delayed failure in the weeks or months following an event [*Gaunt and Coetzee*, 2007; *Moodley and Gaunt*, 2012], would cause problems in energy-constrained economies, since the transformers most likely to be affected are generator step-up units and the generator capacity will not be available until the transformer is replaced. In addition to having to replace damaged transformers within the region of the extreme GMD, transformers beyond the region might also be damaged. Units in which damage has been initiated will degrade over weeks or months until they fail, well after the GMD event is over. The failure of these transformers in adjacent regions will increase the pressure on manufacturing replacement transformers.

Indirect upstream and downstream economic effects would also arise outside the directly affected blackout zone, where disruption to supply chain linkages prevents normal economic activities taking place. Inoperability in critical infrastructure sectors is one key way in which disruptions can ripple through the global economy. Consequently, extreme space weather events have the potential to disrupt the production, distribution, and consumption of both goods and services around the world, as demonstrated in *Schulte in den Bäumen et al*. [2014].

If an extreme space weather event occurred that led to electricity transmission grid failure, the immediate direct economic impact would be a loss of power for businesses and consumers within the blackout zone. Figure 1 illustrates the structural relationships between firms within the blackout zone and how this disruption affects value-adding activities upstream and downstream within supply chain linkages. It also demonstrates how this can have both domestic and international supply chain impacts.

For example, within the blackout zone the network operator is unable to provide power for Firm 2a and Firm 2b, halting their production activities. Limited analysis of the economic impact of space weather has been undertaken and has often only focused on this first-order impact within the blackout zone [e.g. *Barnes and Dyke*, 1990]. The economic impact of space weather is often quoted in the literature [see *Bolduc*, 2002 or *Space Studies Board*, 2008], but it is not clear if these estimates include second-order indirect impacts.

However, in reality upstream supply chain effects take place outside of the blackout zone as Firm 1a and Firm 1b have lower demand for the goods and services that under normal conditions they would sell to Firm 2a/2b. Moreover, downstream effects mean that Firm 3a and Firm 3b do not have the necessary goods and services required for their production processes, potentially halting their activities despite the fact that they are not in the blackout zone. For example, the 2011 earthquake and tsunami caused direct devastation to Japan and also disrupted downstream industries around the globe because of Japan's pivotal role in international manufacturing. To understand the total impact of an extreme space weather event on the electricity grid, one must use an approach that is able to capture these direct and indirect economic effects.

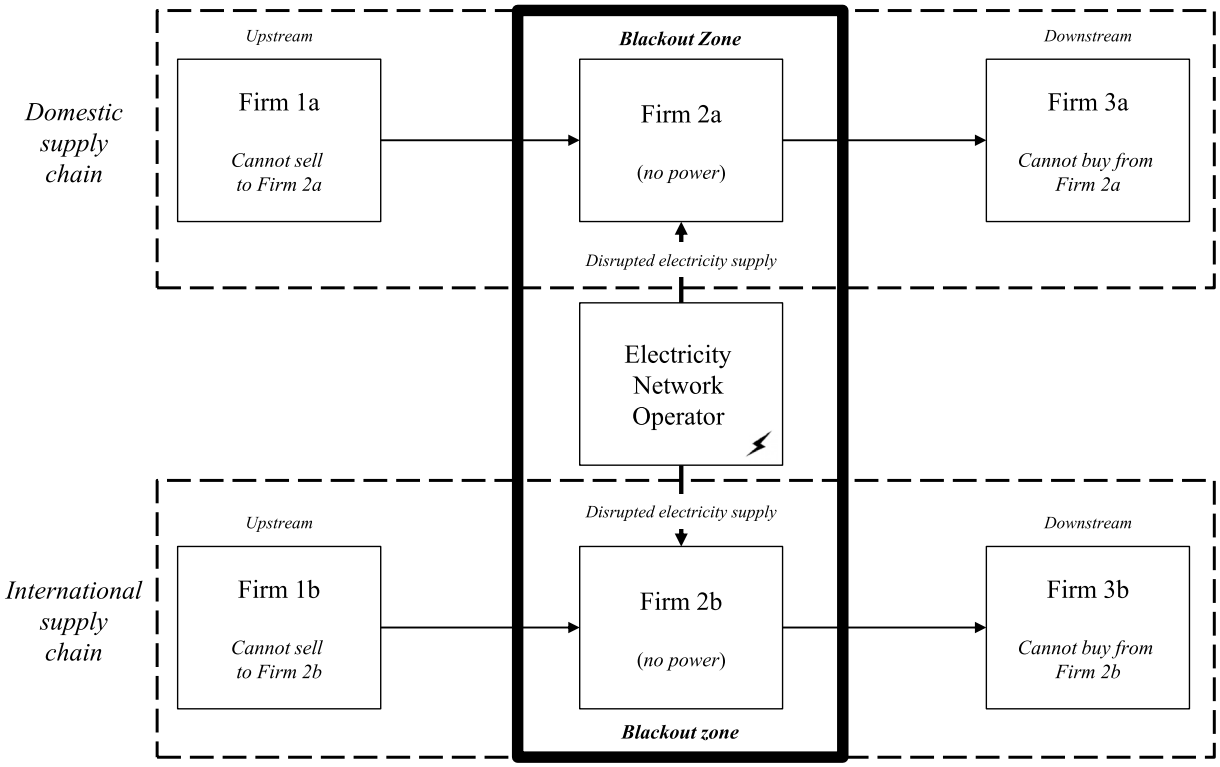

Figure 1. Illustrating the structural relationships in upstream and downstream supply chains.

Finally, while economic cost estimates of potential extreme space weather events are regularly mooted by government and industry, it is not always easy to identify the methodology actually used to assess this economic loss. Transparency is vital for ensuring robust decision making in government and industry, making clear assessment of these potential costs very important. In light of this, we now present our methodology.

2. Methodology

In order to calculate the economic impact, we need to define the region on the ground affected by the storm. To do this, we have set up four different scenarios that depend on the geographical location of the blackout zone, enabling us to explore the sensitivity of the economic loss to electricity failure in different states.

The methodology presented here flows sequentially through the following main steps: (1) determining blackout zone by scenario; (2) calculating state-level direct economic impact from production disruptions; (3) aggregating state-level direct economic impact to national-level sector-specific impact; and (4) estimating indirect domestic and global economic impact.

Step 1: Determining blackout zone by scenario. To make accurate predictions of GIC by region, one normally requires considerable information on geomagnetic variations in the region as well as shallow and deep-Earth ground conductivity, along with asset-level network information for the electricity transmission grid. Unfortunately, much of the asset information is proprietary or is not readily available. In the absence of comprehensive asset data, which would allow integration of a spatial power sector model into the analysis, we apply various assumptions relating to the electricity transmission network. The blackout zone is parametrized by using data from previous events.

The 1989 Quebec GMD is best known for the failure of the Hydro-Quebec power system, but its effects were detected in other power systems too. Figure 2 shows the variation of the magnetic field during the GMD during 13–14 March 1989, as measured at the Ottawa, Canada, magnetic observatory in the region of the Hydro-Quebec network that failed in the early morning when the dH/dt measurement at Ottawa was approximately 435 nT/min. Later in the day, when measurements between 450 and 560 nT/min were

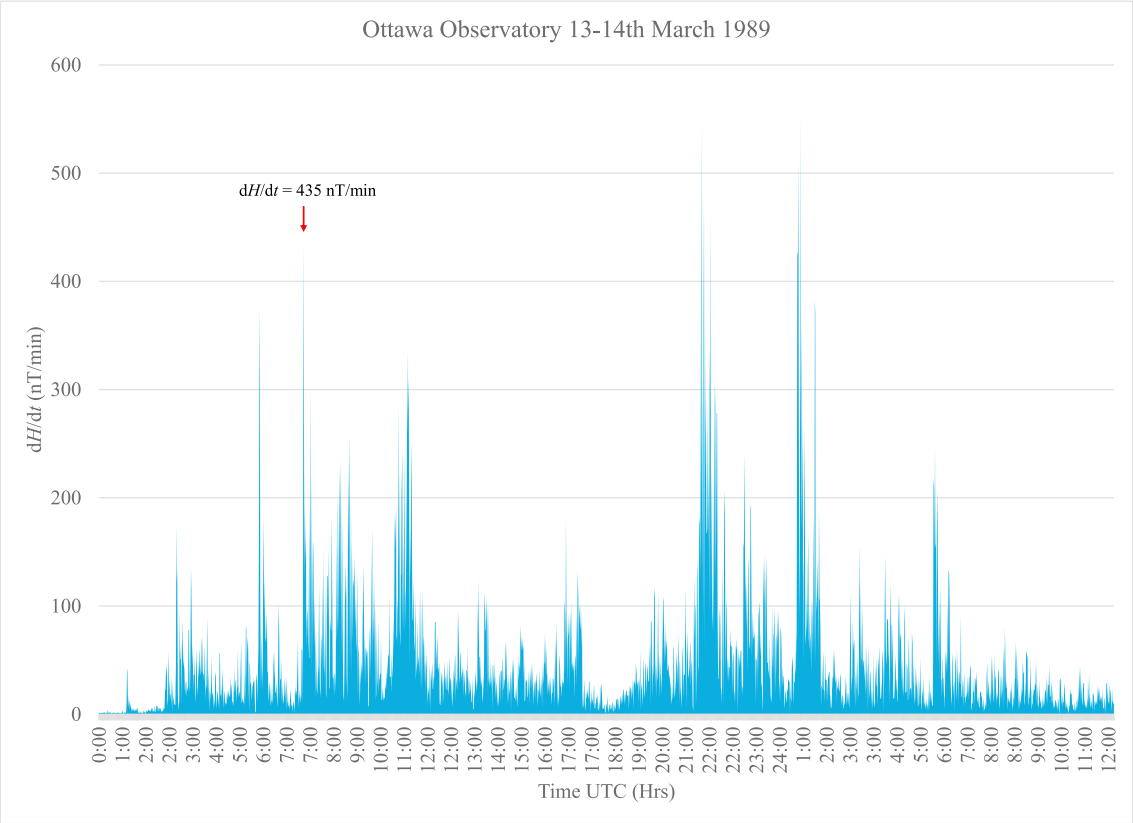

Figure 2. Ottawa d*H*/d*t* 13–14 March 1989 [*Natural Resources Canada*, 2016].

recorded at Ottawa, disturbances in other power systems south and west of Ottawa occurred without progressing to complete voltage collapse, though several large transformers were damaged. The various events during the Quebec GMD illustrate how combinations of GMD magnitude, regional geology, transformer design, and network topology and loading lead to variability in the power system response to a disturbance. As illustrated by large area blackouts in North America, Europe, Brazil, and India, large modern networks appear to be less robust to disturbances than 30 years ago, so d*H*/d*t* values of 450–600 nT/min, well below the values expected in extreme events, must be expected to initiate equipment damage or power system voltage collapse, or both.

During a major magnetic storm, the ring current intensifies leading to a rapid decrease in the *Dst* index and a recovery phase that may last a few days or even longer. During the storm, multiple substorms can also take place [*Tsurutani et al*., 2015] leading to large electrical currents flowing into the ionosphere, through the ionosphere, and out into space again. The rapid changes in these currents in the ionosphere lead to the large d*B*/d*t* values that induces GIC at the surface. These currents flow in an enhanced channel of electrical conductivity created by particle precipitation and are known as the auroral electrojets and are measured by the *AE* index. Therefore, for the purposes of our model we assume that the region of maximum d*B*/d*t* occurs inside the auroral electrojet.

Pulkkinen et al. [2012] have compared the values of d*B*/d*t* for the horizontal geoelectric field measured during the large storms of 13–14 March 1989 and 29–31 October 2003. They conclude that the auroral region reached further equatorward in 1989 than in 2003 and that, at any time, the latitudinal width of the most intense disturbance in the auroral region is narrow. However, it is not clear from the measurements of the maximum d*B*/d*t* at each location how narrow the latitudinal width is during the substorms. The center of the electrojet is usually located near 72° geomagnetic latitude [*Rostoker and Duc Phan*, 1986]. For relatively large values of *AE* of up to 600 nT the region moves equatorward to 65°, but the latitudinal width of the region remains almost constant at 5.5°–6° [Ibid.]. Hence, in our model we assume a latitudinal width corresponding to 5.5° inside which d*B*/d*t* can be very large and where the power grid below can be affected. We assume that

d*B*/d*t* for our extreme event scenarios is large enough to affect the power grid across the whole 5.5° GMD footprint. Structures of such extent can be seen in *Pulkkinen et al*. [2015].

Extreme value analysis shows that the *AE* index can be as large as 4056 nT [*Nakamura et al*. 2015] and that d*B*/d*t* could be larger at subauroral latitudes than auroral latitudes [*Wintoft et al*. 2016]. Following the trend observed by *Rostoker and Duc Phan* [1986], this suggests that the electrojet should move to even lower latitudes. Observations from ground-based magnetometer chains suggest that the auroral electrojet extended down to 54°–55° geomagnetic latitude during the intense magnetic storm of May 1992 where *Dst* reached −300 nT [*Feldstein et al*., 1997]. For much larger storms, it is very difficult to assess the latitude to which the electrojet might reach. *Pulkkinen et al*. [2012] suggest 50°, with the magnitude of the geoelectric field dropping significantly between 40° and 50°. Visible aurora is another indicator, and during the 1859 Carrington Event, the aurora was observed as low as 20° [*Silverman*, 2008]. Moreover, during the storm of 4 February 1872 the aurora was observed as low as 10° [Ibid.]. However, there can be a large difference between (i) the location of the observer and the actual latitude of the aurora, (ii) the location of the aurora and the largest d*B*/d*t*, and (iii) the type of aurora, for example, a red aurora has been observed over Japan as low as 45° geomagnetic latitude [*Shiokawa et al*., 2013] but is not usually associated with rapidly changing currents. In addition, we would expect particle precipitation contributing to the electrojet to lie outside the plasmapause, and typically this was eroded to an altitude of around 3200 km during the 2003 storm suggesting that the electrojet should lie poleward of 35°.

Given the uncertainties, we assume that in extreme events the auroral electrojet intensifies and moves to lower latitudes in our model. Consequently, the GMD footprint reaches a geomagnetic latitude of 55° ± 2.75° in scenario 1, 50° ± 2.75° in scenario 2, and 45° ± 2.75° in scenario 3. We additionally explore a footprint in scenario 4 (50° ± 7.75°) that is approximately the sum of all other variants, representing the impact of the electrojet moving equatorward and affecting the grid in most states.

We assume that the longitude corresponds to the width of the contiguous United States (excluding Alaska, Hawaii, or other territories under the control of the U.S.) which is approximately 60°. As the Earth rotates all longitudes are affected over a 24 h period so that other countries are also affected. In this analysis, however, we focus purely on the direct impact in the U.S. and how this indirectly affects global supply chains. In reality, as the storm progresses and the electrojet intensifies and moves to lower latitudes, the regions of the power grid on the ground crossed by the electrojet will be disrupted too and suffer a power outage. In this instance, we do not make any assumptions about the duration of the storm but instead calculate the economic loss per day from a 24 h blackout.

Step 2: Estimating state-level direct economic impact from production disruptions. State-level population estimates are obtained from the *U.S. Census Bureau* [2014]. Data are also used from the *U.S. Census Bureau* [2010] on the center of the population and are converted from geographical coordinates to 2016 geomagnetic coordinates using the IGRF-12 calculator [*Thébault et al*., 2015]. A state is included in the scenario if the weighted population center lies within the GMD footprint for each scenario (see Figure 3). In engineering terms, this approach makes an assumption that the north-south connection of networks has a limited effect; this is not entirely valid, such as in California, a state not included in the GMD footprint although significantly dependent on electricity from neighboring states included in S2, S3, and S4. Similarly, in economic terms some significant industrial areas may be excluded from the analysis due to the location of the weighted population center. California is another good example as it lies outside all GMD footprints due to the weight of Los Angeles and San Diego in the south. In reality, the San Francisco bay area may be affected in some scenarios. However, the currently available gross domestic product (GDP) statistics by industrial sector constrain the analysis from being possible at this level of disaggregation. Figure 3 illustrates the blackout zone resulting from the GMD footprint.

It is assumed that every member of the population is an electricity customer; therefore, the number of electricity customers is equal to the total population of a state. Moreover, a key assumption of the analysis is that all economic activities are dependent on electricity; therefore, states included in each scenario undergo 100% blackout. Thus, when this 100% blackout takes place there is a 100% loss in state GDP. Hence, the analysis presents an upper bound on the potential macroeconomic loss from an extreme space weather event, but is still only a proportion of the potential cost as lost value from perishable products, damage to fixed capital equipment, and any subsequent civil unrest due to the blackout are not included in this assessment.

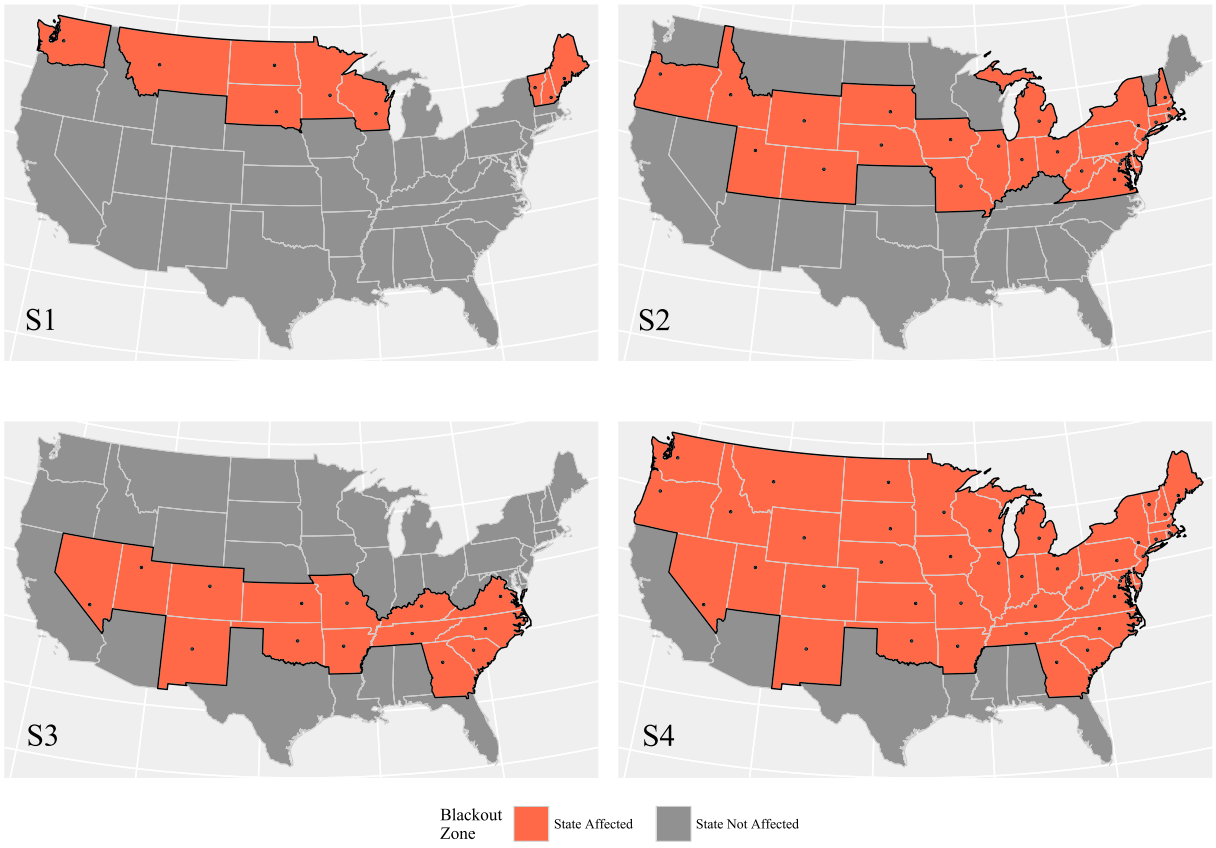

Figure 3. Blackout zone by scenario variant.

The estimation of direct costs consequently provides insight into the loss in sales revenue suffered by businesses in all economic sectors within the geographically affected area of the storm. This step is calculated using real gross domestic product (GDP) data by state [*Bureau of Economic Analysis*, 2011] for 20 broad industrial groups available from the U.S. Bureau of Economic Analysis. The direct economic cost is therefore the lost economic activity proportional to the state GDP under business-as-usual conditions. The data are reported in the 2012 North American Industry Classification System (NAICS). To align with the most recent World Input-Output Database (WIOD) statistics [*Timmer et al.*, 2015] used in the next steps of the method, 2011 data are selected for the analysis [*World Input-Output Database*, 2016]. Some minor variance exists between disaggregated state-level GDP estimates and the aggregate economic output in the WIOD tables, due to differences in national accounting methods.

Step 3: Aggregating state-level direct economic impact to national-level sector-specific impact. Once state-level production loss has been estimated, we aggregate this by economic sector to reflect the daily direct economic impact nationally. Once complete, we have to address the fact that the 2012 NAICS do not identically map to the sectoral categorization system used in the WIOD data. In this case a concordance table is used to map the relevant NAICS sectors to the WIOD sectoral categorization which is based on the NACE (Nomenclature statistique des Activités économiques dans la Communauté Européenne) revision 1 (corresponding to the International Standard Industrial Classification revision 3) [*Dietzenbacher et al.*, 2013] (see supporting information). Due to minor differences in national account methodologies between the state-level GDP data and aggregate WIOD data, we take the share for each state sector rather than the absolute value.

The underlying data required to perform the analysis takes the form of a balanced Multi-Regional Input-Output (MRIO) table, specifically, the 2011 MRIO table from the WIOD, which characterizes interdependencies between 40 countries (and an aggregate Rest of World region) and 35 economic sectors [*Timmer et al.*, 2015]. These data are derived from National Accounts, Supply and Use Tables, and International Trade Statistics.

Although only a recent development in the field of Input-Output (IO) research, there are now several providers of MRIO data with global coverage (for a comparison of available databases see *Tukker and Dietzenbacher* [2013], *Inomata and Owen* [2014], or *Moran and Wood* [2014] for analysis). However, WIOD places a relatively high reliance on official national accounts statistics (rather than computational algorithmic estimation techniques) and provides the greatest transparency over underlying data sources and methodologies used to construct the tables. Hence, the WIOD is one of the most frequently utilized databases in the literature [*Baldwin and Lopez-Gonzalez*, 2015; *Johnson*, 2014; *Kucukvar et al*., 2015; *Fujii and Managi*, 2015]. Once the concordance table has been utilized, the direct economic loss is shown relative to the NACE (revision 1) categorization at the national level.

Step 4: Estimating of indirect domestic and global economic impact. We employ an IO approach to calculate indirect economic costs. Using a system of linear equations, the IO framework represents each economic sector's dependence (as monetary flows) on all other sectors of the domestic and global economy. This is a useful tool because it enables the interdependencies between economic sectors to the quantified, thereby providing insight into the upstream and downstream supply chain linkages in the production and consumption of goods and services. An in-depth overview of the IO approach can be found in *Miller and Blair* [2009]. Using IO data, we are able to explore the impact of a blackout on the economy and how lost value propagates via economic interdependencies between industrial sectors. This can be addressed using the conventional Leontief open model, given by

$$\mathbf{x} = (\mathbf{I} - \mathbf{A})^{-1}\mathbf{y} \tag{1}$$

where **x** is a vector of sector total outputs, **y** is a vector of final demand for the goods and services produced by each sector, **I** is an identity matrix, and **A** is a matrix of sector direct requirements (or technical coefficients). Each column of the direct requirements matrix represents a sector's production function of inputs from all other sectors that are needed to make one unit of output. This demand-side model centers on the key assumption that the ratios of a sector's production requirements are fixed; that is, for example, a 10% reduction in the output of a given sector due to a power outage would lead to a 10% reduction in all of its intermediate demands on other sectors. As such, the model explores upstream consequences (or attributions) of a downstream impact (or consumption quantity).

The IO literature also provides a counterpoint for the investigation of downstream consequences, based on the Ghosh open model [*Miller and Blair*, 2009], given by

$$\mathbf{x} = \mathbf{v}(\mathbf{I} - \mathbf{B})^{-1} \tag{2}$$

where **v** is a vector of value added in each sector and **B** is a matrix of sector direct sales. Each row of the direct sales matrix represents the distribution of a unit of output from one sector, across all other sectors (showing production inputs). This supply-side model assumes that the function of production inputs for each sector is consequently fixed; hence, a 10% reduction in the output of a given sector would lead to a 10% reduction in that sector's sales to all other sectors.

Following on with the sequential methodology, we are concerned with assessing the consequences of shocks to the production capacity of different sectors caused by a power outage due to extreme space weather. It is intuitive to consider that a 10% loss in the production capabilities of say the steel sector will have both upstream and downstream consequences. As less product is being produced, there will be fewer units available to sell to purchasing sectors (downstream effects), along with less demand for intermediate product inputs usually used in production (upstream effects).

A novel approach has been developed which combines features of the standard Leontief and Ghosh formulations along with insights into pure linkage measures proposed by *Sonis et al*. [1995]. The approach provides an estimated range of indirect impacts for a disparate set of shocks across sectors; the reported range considers both the optimistic possibility, for the lower bound, that sector shocks align along common supply chains and the conservative possibility, for the upper bound, that shocks are universally misaligned along supply chains.

The indirect loss has also been broken down into the proportion that has taken place either upstream (supply affected) or downstream (demand affected) of a specific sector, as illustrated earlier in Figure 1. Both the

direct loss and the upstream and downstream indirect loss cannot exceed total daily GDP (individually or collectively).

For each sector s experiencing a shock to its production capacity (total output, Δx_s), the upstream impact on the economy $\Delta \mathbf{x}_s^{up}$, that is free from intrasector demands and feedbacks from the rest of the economy, is given by

$$\Delta \mathbf{x}_s^{up} = (\mathbf{I} - \mathbf{A}^*)^{-1} \mathbf{A}_{:s} \Delta x_s \tag{3}$$

where $\mathbf{A}^*$ is a submatrix of the technical coefficients matrix where the row and column ascribed to sector s have been stripped out, and $\mathbf{A}_{:s}$ is a column subvector of the technical coefficients matrix where the row ascribed to sector s and columns ascribed to all other sectors have been stripped out (i.e., the colon symbol denotes all sectors except sector s).

Similarly, the downstream impact on the economy $\Delta \mathbf{x}_s^{down}$ is given by

$$\Delta \mathbf{x}_s^{down} = \Delta x_s \mathbf{B}_{s:} (\mathbf{I} - \mathbf{B}^*)^{-1} \tag{4}$$

where, $\mathbf{B}^*$ is a submatrix of the direct sales matrix where the row and column ascribed to sector s have been stripped out, and $\mathbf{B}_{s:}$ is a column subvector of the direct sales matrix where the column ascribed to sector s and rows ascribed to all other sectors have been stripped out.

Finally, feedback impact on sector s from the rest of the economy $\Delta \mathbf{x}_s^{fb}$ is given by

$$\Delta \mathbf{x}_s^{fb} = \mathbf{A}_{s:} (\mathbf{I} - \mathbf{A}^*)^{-1} \Delta \mathbf{x}_s^{up} = \Delta \mathbf{x}_s^{down} (\mathbf{I} - \mathbf{B}^*)^{-1} \mathbf{B}_{:s} \tag{5}$$

Defining the direct total output shock vector as $\Delta \mathbf{x}^{dir}$, we can now specify the optimistic lower bound $\Delta \mathbf{x}^{total,lb}$ and conservative upper bound $\Delta \mathbf{x}^{total,ub}$ for total (direct and indirect) impacts as follows

$$\begin{aligned} \Delta \mathbf{x}^{total,lb} &= \min_s \left[\Delta \mathbf{x}^{dir}, \min_s \Delta \mathbf{x}_s^{up}, \min_s \Delta \mathbf{x}_s^{down}, \min_s \Delta \mathbf{x}_s^{fb} \right] \quad \Delta \mathbf{x}^{total,ub} \\ &= \Delta \mathbf{x}^{dir} + \sum_s \Delta \mathbf{x}_s^{up} + \sum_s \Delta \mathbf{x}_s^{down} + \sum_s \Delta \mathbf{x}_s^{fb} \end{aligned} \tag{6}$$

Using this approach, we are able to rank those economic sectors that feature the largest direct and indirect loss in economic output as a consequence of the extreme space weather scenario variants. These estimates are approximate, as loss from production disruption does relate to the size of firm inventories and the degree of substitution that can take place with other production inputs [*Hallegatte*, 2012]. In recent years, the proliferation of "Just-in-Time" and "Lean" manufacturing strategies to reduce inventory costs has increased the vulnerability of indirect supply chain loss. This analysis provides insight that can be used for supporting decision making in resilience planning, as well as helping to bolster private and public investment into protecting interdependent critical infrastructure assets with the aim of avoiding catastrophic events, providing the risk is fully understood. Now the method has been outlined, the results will be presented in section 3.

3. Results

This section reports the results in terms of the direct and indirect economic loss to U.S. industrial sectors. All monetary units are in 2011 U.S. dollars. In terms of total loss, the S1 scenario at $55° \pm 2.75°$ geomagnetic latitude affected 8% of the U.S. population and caused an economic loss to the U.S. economy of $6.2 billion per day (15% of daily U.S. GDP). This is supplemented by an international daily loss of $0.8 billion. The S1 scenario is considerably lower than the other scenarios, as only the northernmost states were actually affected, as discussed in greater detail later. In the S1 scenario, the largest loss was seen in Washington State, followed by Wisconsin and Minnesota. The remaining states have relatively little economic activity. Figure 4 illustrates the blackout zone by scenario variant in relation to the number of daily electricity customer disruptions and daily lost state-level GDP.

In the S2 scenario ($50° \pm 2.75°$ geomagnetic latitude) a considerable proportion of industrial production was affected, along with 44% of the population. Disruption in key states including New York, Illinois, Pennsylvania, Ohio, and Michigan led to an economic loss to the U.S. economy of $37.7 billion per day (91% of daily U.S. GDP). The international daily loss reached $4.8 billion. As illustrated in Figure 4, although there is significant

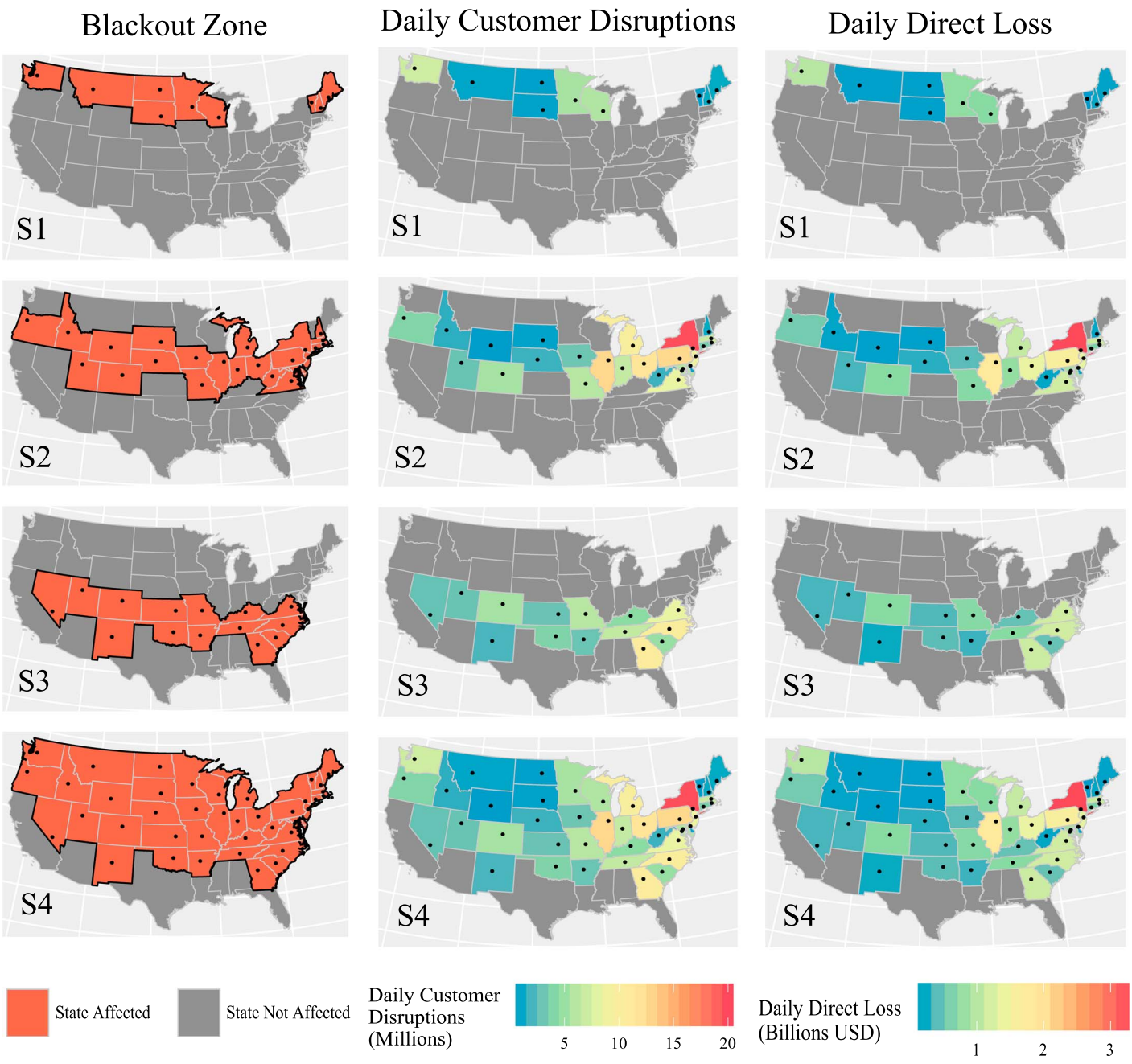

Figure 4. Blackout zone, daily customer disruptions, and daily lost GDP by scenario.

disruption across the states in the northeast and Midwest regions, New York is most badly affected because it is such a key contributor to the U.S. economy.

The S3 scenario (45° ± 2.75° geomagnetic latitude) affected 23% of the U.S. population leading to an economic loss of $16.5 billion per day (40% of daily U.S. GDP). The international economic loss incurred was $2.2 billion per day. The largest number of customer disruptions are in Georgia, North Carolina, Virginia, and Tennessee.

In the much larger S4 scenario (50° ± 7.75° geomagnetic latitude), 66% of the population were affected. This leads to an estimated potential economic loss of $41.5 billion per day to the U.S. economy (100% of daily U.S. GDP), combined with a daily loss to the global economy of $7 billion.

Table 1. Loss by Scenario Variant

Scenario Variant	U.S. Population Affected	U.S. Direct Loss ($bn)	U.S. Indirect Downstream Loss ($bn)	U.S. Indirect Upstream Loss ($bn)	Global Indirect Downstream Loss ($bn)	Global Indirect Upstream Loss ($bn)	Global Total Macroeconomic Loss ($bn)
S1	8%	$3.2	$1.6	$1.4	$0.5	$0.3	$7
S2	44%	$19.7	$9.3	$8.7	$2.7	$2.1	$42.4
S3	23%	$8.6	$4.2	$3.7	$1.3	$0.9	$18.7
S4	66%	$28.2	$6.1	$7.2	$4	$3	$48.5

Table 1 breaks down the economic loss for each scenario into the direct and indirect economic impact. Indirect effects are segmented into upstream or downstream economic loss.

Other studies estimated U.S. daily economic loss to be between $25 billion [*Schulte in den Bäumen et al*., 2014] and $37.5 billion per day [*Lloyd's*, 2013]. The results gained here are broadly comparable; however, this study explores different blackout zones. For example, in the S1 scenario where there is less auroral shift, only 12 of the most northerly states are affected. These are generally less populated, producing a smaller loss. The S2 scenario produces the second largest economic loss due to the size and economic importance of the states affected which include New York (including New York City), Illinois (including Chicago), and Pennsylvania (including Philadelphia). The S4 scenario is much larger than previous studies. A key contribution of this paper is the insight provided from exploring the geographical location of the blackout zone and the resulting sensitivity of the economy.

Figure 5 compares the direct and indirect economic loss across each scenario by industrial sector. Manufacturing sees the largest direct economic loss in all variants (S1, $0.5 billion; S2, $2.4 billion; S3, $1.2 billion; and S4, $3.7 billion). This is partly because it is one of the largest overall sectors in terms of economic output. This type of industrial activity is highly clustered in comparison with other, more ubiquitously distributed activities such as Real estate activities, or Health care and social assistance. Finance and insurance is more affected in S2 when the event causes disruption in New York, Chicago, and Philadelphia. Across the scenarios approximately 49% of lost output occurred through direct loss in the U.S., and for every $9 lost by private industry, approximately $1 was lost by the Government sector.

Indirect loss occurs to the U.S. economy due to the interdependencies that exist between economic sectors, resulting in second-order impacts taking place outside of the blackout zone. Total domestic indirect economic loss reached $3 billion (bn) in S1, $18 bn in S2, $7.9 bn in S3, and $13.3 bn in S4. The larger direct loss in S4 led to a smaller indirect loss, as more firms were located within the blackout zone. In terms of industrial sectors, manufacturing sees the largest total indirect loss within the U.S. (S1, $0.5 bn; S2, $2.8 bn; S3, $1.3 bn; and S4, $1.5 bn). Again, this is logical based on the size of this sector, along with the fact that these activities can rely on many physical inputs from across the economy leading to the largest upstream indirect loss. Government had the second largest upstream indirect loss. In terms of indirect downstream loss, the sectors most affected were Manufacturing; Finance and insurance; and Professional, scientific, and technical services.

Across the scenarios approximately 39% of lost output occurred through indirect domestic U.S. loss, and much like the direct impact, for every $9 lost by private industry indirectly, approximately $1 was lost by the Government sector.

Figure 6 illustrates the results for each of the scenarios for the most affected nations in terms of indirect upstream and downstream economic loss. China had the largest total indirect economic loss from each of the scenarios per day (S1, $0.1 bn; S2, $0.58 bn; S3, $0.27 bn; and S4, $0.86 bn), followed closely by Canada (S1, $0.1 bn; S2, $0.56 bn; S3, $0.26 bn; and S4, $0.83 bn) and then Mexico (S1, $0.06 bn; S2, $0.35 bn; S3, $0.17 bn; and S4, $0.52 bn). China is most badly affected because of its strong trading relationship with the U.S. As Canada and Mexico trade more with the U.S. due to their geographically proximate positions, they also suffered a large above average economic loss. China, Canada, and Mexico see larger downstream effects, indicating that these countries provide a greater proportion of raw materials and intermediate goods and services, used in production by U.S. firms.

The next group of countries seeing similar economic loss is Japan, Germany, and the UK. In S3 the economic loss suffered by these countries is slightly different. This is due to the distribution of industrial activity by state and how disruption by sector aggregates to the national level and affects international supply chain linkages

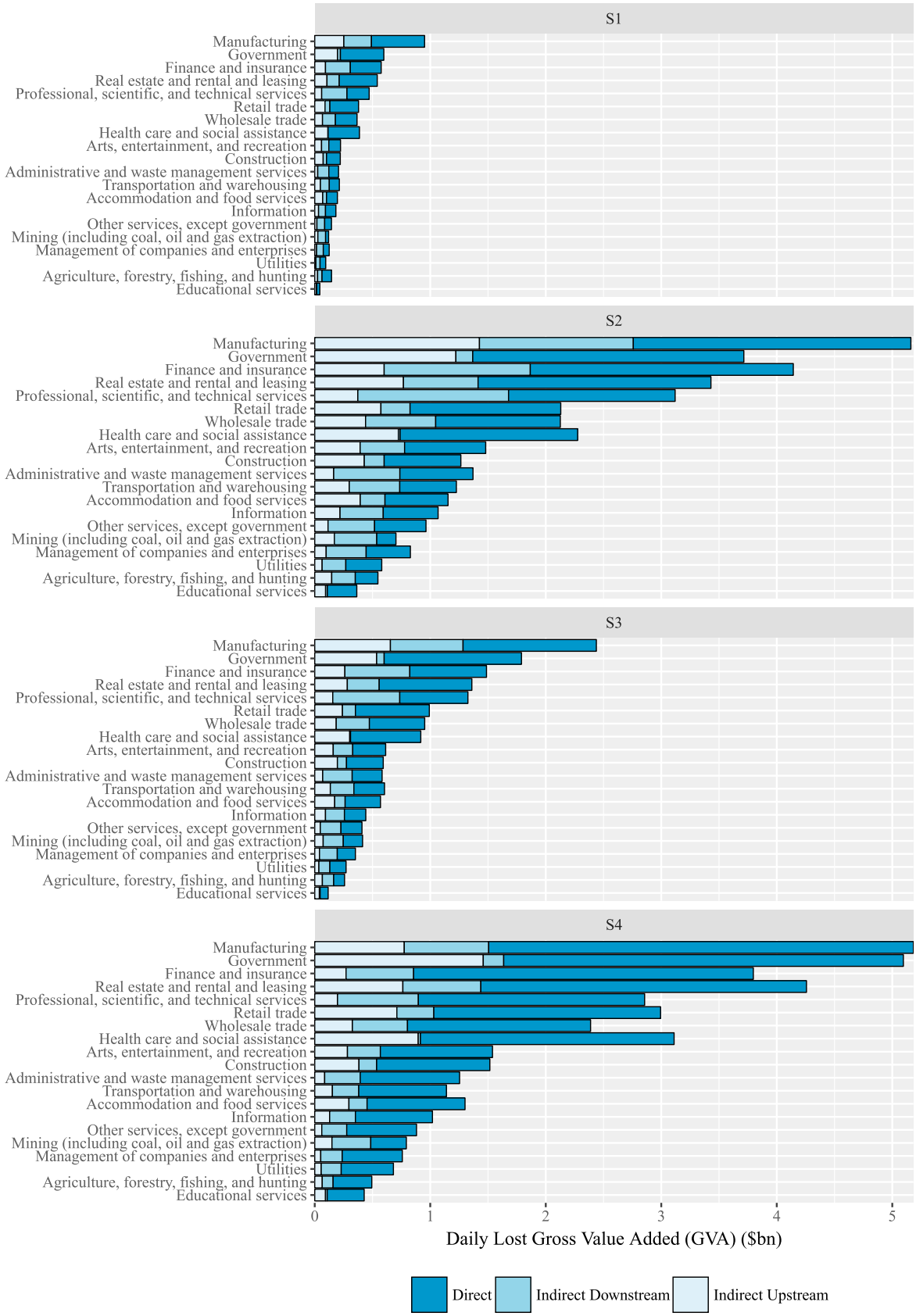

Figure 5. Daily direct and indirect loss to the U.S. by industrial sector.

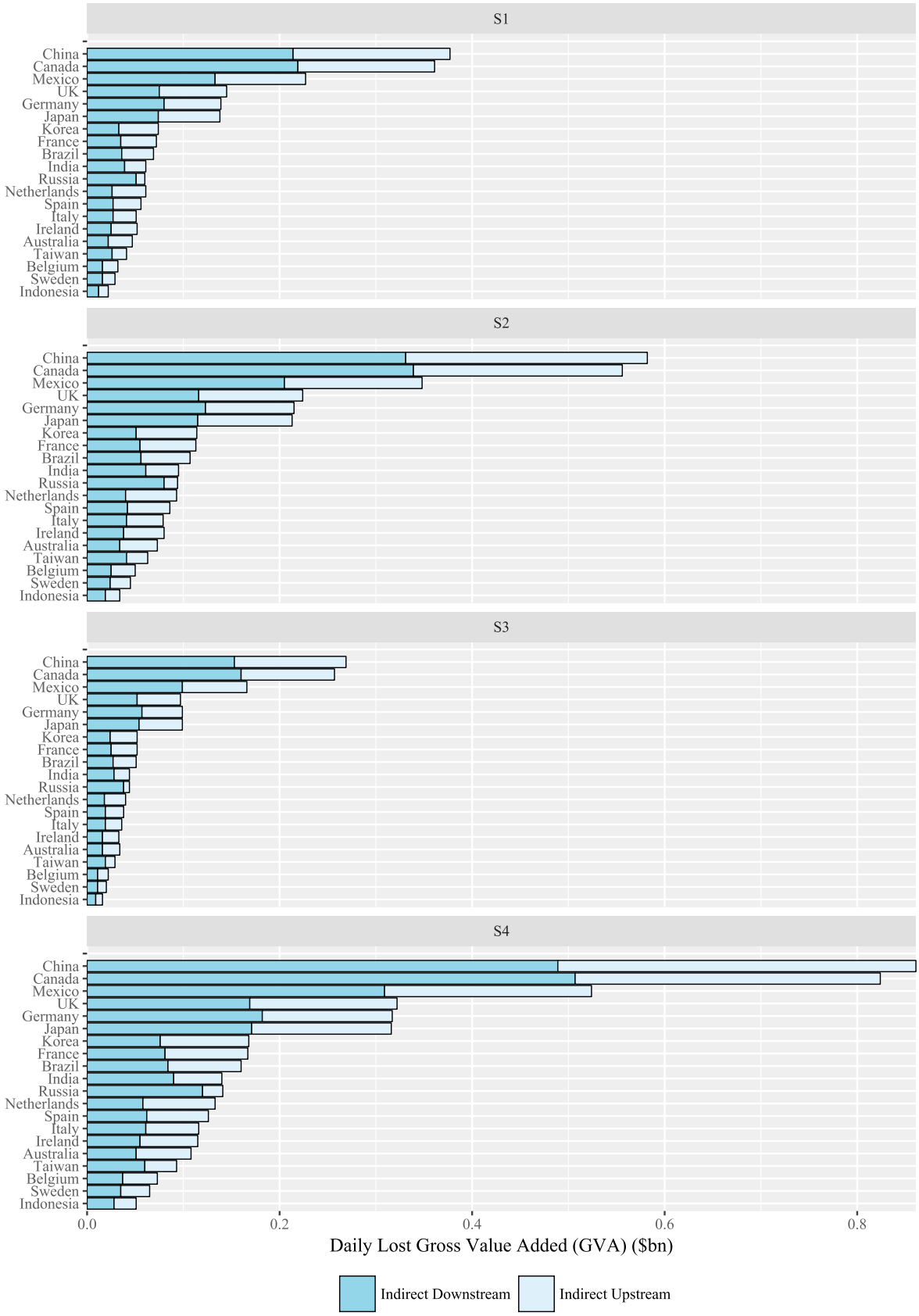

Figure 6. Daily global indirect loss via international supply chains.

between countries. The UK ranks slightly lower on S3 when the power outage does not affect major states such as New York or Chicago. However, in S1 and S2 the UK moves up two places due to disruption in key sectors such as Manufacturing and Finance and insurance. South Korea, Germany, and France all feature comparatively large loss when ranked against other nations, due to their manufacturing sectors, which is logical given their dominance in such industries as electronic goods, car manufacturing, and aircraft manufacturing, respectively. On average, a total of approximately 12% of lost economic output occurred through indirect global loss outside of the U.S. These findings will now be discussed.

3.1. Discussion

It is important to recognize that the true economic impact of an extreme space weather event stretches far beyond simply the value of the damaged transmission assets, or unsold electricity, or even those firms disrupted without power within the blackout area. Of the total economic loss estimated here, indirect domestic lost value represented 39% of the entire event on average across each scenario, and international lost value on average represented a further 12%. In other words, if an analyst only counted the costs incurred directly from an extreme event within the blackout zone, as has been done in previous studies, this only represents roughly 49% of the macroeconomic cost. Hence, capturing all indirect effects is essential in order to begin to have a more comprehensive understanding of the *true potential cost* of extreme space weather.

We see a number of benefits that can result from this work. First, it is relevant for government and emergency planning agencies to be able to understand the economic and critical infrastructure sectors that may be affected under these conditions. This supports the decision-making processes associated with allocating limited resources. There is likely to be desirability to preference those sectors that cause the largest loss in economic output. Second, in terms of the relevance of these findings for private industry, the results can be of use to both network operators of critical national infrastructure, as well as those financially responsible for any cost incurred as a result of interruptions. For example, in the insurance industry firms must either exclude risk arising from space weather events or price the risk into the policies they offer.

The scenarios outlined in this research prove a useful tool in a number of ways. Insurance firms are able to examine their customer exposure to extreme space weather events based on the property, casualty, business continuity, and supply chain policies that they insure. The scenarios presented here prove a useful stress test tool for exposure management because it shows the sector-specific economic loss that can result from different extreme space weather events. Indeed, given that in the UK General Insurance Stress Test 2015 undertaken by the PRA provides relatively little direction regarding the stress test for this threat, information provided here can help to direct those required to undertake such a task.

The modeling carried out in this analysis indicates two areas in which the assumptions, while based on the best information available, require further research. The first is in understanding how much redundancy lies in the power grid. A power system shutdown initiated by equipment failure or automatic protection responses could reduce catastrophic damage to transformers and allow the networks to be restored within days. Outside these areas, damage initiated by GIC might have longer-term, though less extreme, effects. The details of electrical grid collapse and equipment damage require a much better understanding of the behavior of different types (and designs) of transformers and the effectiveness of the various approaches to mitigation. Second, the economic model is subjected to a relatively short-term economic disruption; therefore, there needs to be more research into the available inventories in different industries and the degree of substitution in production inputs, as this affects economic loss estimation.

The economic impact assessment of multiday, multiregional extreme space weather events is an area of further research that needs to be addressed. A multiday extreme event is likely to cause direct disruption of more than one region of the world. Even the effects of multiple substorms during the Quebec storm caused smaller disturbances at different times in other parts of North America and in the United Kingdom. Therefore, disturbances on day 2 or 3 of an extreme event, additionally affecting Europe as well as the U.S. (and even Australasia in the Southern Hemisphere), would incur much greater economic loss than modeled in this paper. As well as expanding this analysis to other nations, it may also be important to assess the implications of intense microscale and mesoscale (100–1000 km) geomagnetic events [*Pulkkinen et al.*, 2015; *Ngwira et al.*, 2015] where disruption is far more localized, should the available economic statistics support this level of granularity. However, in this endeavor we do not yet have a scientifically robust way to link

together extreme space weather, the expected response of the power grid exposed to GIC, and finally how this may lead to lost direct and indirect economic value. One way to achieve this is by ensuring that there is more collaborative work between space physicists, electrical engineers, and economists. No doubt that the lack of data, particularly of transformer and network response and the costs of interruptions, is holding back further research in the field.

By exploring the impact of space weather in monetary terms, this work enables interpretation by a wider audience with a responsibility to understand this threat but who perhaps do not have a background in space physics, geophysics, or electrical engineering. It has already been identified that there are issues in portraying aspects of extreme space weather to the public, government, and business, especially as the infrequent nature of these events and the technical language used to explain key aspects of this subject can be challenging to communicate. Converting the potential impacts into economic estimates makes this especially interpretable to economists, actuaries, and senior corporate management. Indeed, the research presented here can be used as a discussion device between insurance underwriters, exposure analysts, and chief risk officers in the insurance industry, as it highlights the potential economic consequences associated with extreme space weather, given that there is a requirement for them to understand this threat.

Acknowledgments
The authors acknowledge partial financial support from American International Group during the research and especially thank Brad Fischtrom, Siddhartha Dalal, and their team for providing useful comments and insights as the research progressed. We also thank attendees of the workshop held at the Cambridge Judge Business School in July 2015. Three anonymous reviewers are acknowledged for providing useful comments and feedback on the paper. Oughton was partially supported by the UK Engineering and Physical Science Research Council under grant EP/N017064/1: Multiscale InfraSTRucture systems AnaLytics. Horne and Thomson would like to acknowledge the support of the Natural Environment Research Council (NERC). This paper is published by permission of the Executive Director, British Geological Survey (NERC). The authors have no conflicts of interests. While undertaking this work Jennifer Copic provided invaluable research assistance and Tamara Evans kindly proofread various versions of the manuscript. We also thank senior members of the Cambridge Centre for Risk Studies for their ongoing support, including Simon Ruffle, Andrew Coburn, Danny Ralph, and Michele Tuveson. Specialist subject matter guidance was also provided by David Boteler, Helen Mason, and Mark Clilverd. Data used in this analysis are available from the U.S. Bureau of Economic Analysis (http://www.bea.gov/), U.S. Census Bureau (https://www.census.gov/), and World Input-Output Database (http://www.wiod.org/new_site/home.htm). The data leading to the conclusions drawn in this paper have been provided in the supporting information. The code required to reproduce the analysis is available from the authors upon request (e.oughtonb@jbs.cam.ac.uk).

4. Conclusions

This paper explored the direct and indirect daily economic costs associated with different scenarios of extreme space weather on mainland U.S., focusing on the upstream and downstream supply chain impact. The total daily economic loss to the U.S. economy associated with a storm within $55° \pm 2.75°$ geomagnetic latitude (S1) was \$6.2 bn (15% of daily U.S. GDP). This is predicated on approximately 8% of the population being left without power. This is supplemented by an indirect loss to the global economy via supply chain linkages with other nations of \$0.8 bn per day. The total daily economic loss to the U.S. economy associated with a storm within $50° \pm 2.75°$ geomagnetic latitude (S2), leaving 44% of the U.S. population without power, was \$37.7 bn (91% of daily U.S. GDP). The indirect loss to the global economy via supply chain linkages with other nations is a further \$4.8 bn per day. The S3 scenario with a blackout zone of $45° \pm 2.75°$ geomagnetic latitude (S3) left 23% of the population without power. The total daily economic loss to the U.S. economy was \$16.5 bn (41% of daily U.S. GDP), and the indirect loss to other nations totaled \$2.2 bn. Finally, the S4 scenario ($50° \pm 7.75°$ geomagnetic latitude) affected 66% of the U.S. population leading to an estimated potential economic loss of \$41.5 billion per day to the U.S. economy (100% of daily U.S. GDP), combined with a daily loss to the global economy of \$7 billion.

A key finding was that the direct economic cost incurred from disruption to electricity within the blackout zone was only a fraction of the total cost for those scenarios explored. On average in this study, only 49% of the total economic loss took place in the area affected by the storm, with a further 39% being lost indirectly in the U.S. outside of the blackout zone. A total of 12% of the impact took place internationally. Therefore, there is a great need when undertaking cost-benefit analysis of space weather forecasting and mitigation investment to consider the domestic and global indirect costs that could accrue via supply chains disruption; otherwise, the potential total cost is not being correctly represented.

However, this analysis focused only on the U.S., when in reality we could be susceptible to a multiday, multiregional extreme space weather event. As a consequence, there is a need to undertake further economic impact assessment including Europe and East Asia, with multiple blackout zones, in order to understand the potential global cost associated with this threat.

References

Anderson, C. W., J. R. Santos, and Y. Y. Haimes (2007), A risk-based input–output methodology for measuring the effects of the August 2003 northeast blackout, *Econ. Syst. Res.*, *19*(2), 183–204.

Baker, D. N., X. Li, A. Pulkkinen, C. M. Ngwira, M. L. Mays, A. B. Galvin, and K. D. C. Simunac (2013), A major solar eruptive event in July 2012: Defining extreme space weather scenarios, *Space Weather*, *11*, 585–591, doi:10.1002/swe.20097.

Balan, N., R. Skoug, S. Tulasi Ram, P. K. Rajesh, K. Shiokawa, Y. Otsuka, I. S. Batista, Y. Ebihara, and T. Nakamura (2014), CME front and severe space weather, *J. Geophys. Res. Space Physics*, *119*, 10,041–10,058, doi:10.1002/2014JA020151.

Baldwin, R. and J. Lopez–Gonzalez (2015), Supply-chain trade: A portrait of global patterns and several testable hypotheses, *The World Economy*, *38*(11), 1682–1721, doi:10.1111/twec.12189.

Banerjee, A., A. Bej, and T. N. Chatterjee (2012), On the existence of a long range correlation in the Geomagnetic Disturbance storm time (Dst) index, *Astrophys. Space Sci.*, *337*(1), 23–32. doi:10.1007/s10509-011-0836-1.

Barbosa, C., L. Alves, R. Caraballo, G. A. Hartmann, A. R. R. Papa, and R. J. Pirjola (2015), Analysis of geomagnetically induced currents at a low-latitude region over the solar cycles 23 and 24: Comparison between measurements and calculations, *J. Space Weather Space Clim.*, *5*, A35, 9.

Barnes, P. R., and J. W. V. Dyke (1990), Economic consequences of geomagnetic storms (a summary), *IEEE Power Eng. Rev.*, *10*(11), 3–4.

Bolduc, L. (2002), GIC observations and studies in the Hydro-Québec power system, *J. Atmos. Sol. Terr. Phys.*, *64*(16), 1793–1802.

Boteler, D. H., R. J. Pirjola, and H. Nevanlinna (1998), The effects of geomagnetic disturbances on electrical systems at the Earth's surface, *Adv. Space Res.*, *22*(1), 17–27.

Bureau of Economic Analysis (2011), Regional Economic Accounts: Real GDP by State (NAICS). [Available at: http://www.bea.gov/regional/downloadzip.cfm, accessed 2016-08-04.]

Cannon, P. S. (2013), Extreme space weather: impacts on engineered systems and infrastructure. Royal Acad. of Eng. [Available at: http://eprints.lancs.ac.uk/id/eprint/64443, accessed 2017-01-06).]

Czech, P., S. Chano, H. Huynh, and A. Dutil (1992), The Hydro-Québec system blackout of 13 March 1989: System response to geomagnetic disturbances, in *Proceedings of Geomagnetically Induced Currents Conference, 8–10 November 1989*, Electr. Power Res. Inst. Rep., Millbrae, Calif.

Department of Energy (2014), *Large Power Transformers and the U.S. Electric Grid*, Depart. of Energy, Washington, D. C.

Dietzenbacher, E., B. Los, R. Stehrer, M. Timmer, and G. de Vries (2013), The Construction of World Input–Output Tables in the Wiod Project, *Econ. Syst. Res.*, *25*(1), 71–98, doi:10.1080/09535314.2012.761180.

Feldstein, Y. I., A. Grafe, L. I. Gromova, and V. A. Popov (1997), Auroral electrojets during geomagnetic storms, *J. Geophys. Res.*, *102*(A7), 14,223–14,235, doi:10.1029/97JA00577.

Fujii, I., T. Ookawa, S. Nagamachi, and T. Owada (2015), The characteristics of geoelectric fields at Kakioka, Kanoya, and Memambetsu inferred from voltage measurements during 2000 to 2011, *Earth Planets Space*, *67*(1), 1–17.

Fujii, H. and S. Managi (2015), Optimal production resource reallocation for CO_2 emissions reduction in manufacturing sectors. , *Global Environ. Change*, *35*, 505–513, doi:10.1016/j.gloenvcha.2015.06.005.

Gaunt, C. T., Coetzee, G. (2007), Transformer failures in regions incorrectly considered to have low GIC-risk, paper presented Power Tech, 2007 IEEE Lausanne, pp. 807–812.

Haimes, Y., and P. Jiang (2001), Leontief-Based Model of Risk in Complex Interconnected Infrastructures, *J. Infrastruct. Syst.*, *7*(1), 1–12. doi:10.1061/(ASCE)1076-0342(2001)7:1(1).

Hallegatte, S. (2012), Modeling the roles of heterogeneity, substitution, and inventories in the assessment of natural disaster economic costs, WPS6047, The World Bank. [Available at http://documents.worldbank.org/curated/en/410441468142479058/Modeling-the-roles-of-heterogeneity-substitution-and-inventories-in-the-assessment-of-natural-disaster-economic-costs, accessed 7 Oct 2016.]

Hapgood, M., et al. (2012), Summary of space weather worst-case environments. Didcot: Science and Technology Facilities Council. [Available at: http://eprints.lancs.ac.uk/64441/, accessed 2015-06-25.]

Inomata, S. and A. Owen (2014), Comparative Evaluation of Mrio Databases, *Econ. Syst. Res.*, *26*(3), 239–244, doi:10.1080/09535314.2014.940856.

Intriligator, D. S., W. Sun, M. Dryer, J. Intriligator, C. Deehr, T. Detman, and W. R. Webber (2015), Did the July 2012 solar events cause a "tsunami" throughout the heliosphere, heliosheath, and into the interstellar medium?, *J. Geophys. Res. Space Physics*, *120*, 8267–8280, doi:10.1002/2015JA021406.

ISGI (2016), ISGI—International Service of Geomagnetic Indices [online]. [Available at http://isgi.unistra.fr/indices_aa.php, accessed 3 Oct 2016.]

JASON (2011), Impacts of severe space weather on the electric grid, JASON, Mclean, Va. [Available at https://fas.org/irp/agency/dod/jason/spaceweather.pdf, accessed 3 Mar 2016.]

Johnson, R. C. (2014), Five facts about Value-Added Exports and Implications for Macroeconomics and Trade Research, *J. Econ. Perspect.*, *28*(2), 119–142.

Kalafatoğlu, E. C., Kaymaz, Z., Moral, A. C., Çağlar, R. (2015), Geomagnetically induced current (GIC) observations of geomagnetic storms in Turkey: Preliminary results, paper presented at the 2015 7th International Conference on Recent Advances in Space Technologies (RAST), pp. 501–503.

Kucukvar, M., G. Egilmez, N. C. Onat, and H. Samadi (2015), A global, scope-based carbon footprint modeling for effective carbon reduction policies: Lessons from the Turkish manufacturing, *Sustainable Prod. and Consumption*, *1*, 47–66, doi:10.1016/j.spc.2015.05.005.

Liou, K., C.-C. Wu, M. Dryer, S.-T. Wu, N. Rich, S. Plunkett, L. Simpson, C. D. Fry, and K. Schenk (2014), Global simulation of extremely fast coronal mass ejection on 23 July 2012, *J. Atmos. Sol. Terr. Phys.*, *121*, 32–41, doi:10.1016/j.jastp.2014.09.013.

Liu, C. M., L. G. Liu, and R. Pirjola (2009), Geomagnetically induced currents in the high-voltage power grid in China, *IEEE Trans. Power Delivery*, *24*(4), 2368–2374.

Liu, L.-G., C.-M. Liu, B. Zhang, Z.-Z. Wang, X.-N. Xiao, and L.-Z. Han (2008), Strong magnetic storm's influence on China's Guangdong power grid, *Chinese J. Geophys.*, *51*(4), 694–699.

Lloyd's (2013), Solar storm risk to the North American electric grid, London: Lloyd's of London.

Marshall, R. A., E. A. Smith, M. J. Francis, C. L. Waters, and M. D. Sciffer (2011), A preliminary risk assessment of the Australian region power network to space weather, *Space Weather*, *9*, S10004, doi:10.1029/2011SW000685.

Marshall, R. A., et al. (2013), Observations of geomagnetically induced currents in the Australian power network, *Space Weather*, *11*, 6–16, doi:10.1029/2012SW000849.

Miller, R. E., and P. D. Blair (2009), Input-output analysis: Foundations and extensions, Cambridge Univ. Press.

Moodley, N., and C. T. Gaunt (2012), Developing a power transformer low energy degradation assessment triangle, in *2012 IEEE Power Engineering Society Conference and Exposition in Africa (PowerAfrica)*, pp. 1–6. doi:10.1109/PowerAfrica.2012.6498647.

Moran, D., and R. Wood (2014), Convergence between the Eora, Wiod, Exiobase, and Openeu's consumption-based carbon accounts, *Econ. Syst. Res.*, *26*(3), 245–261, doi:10.1080/09535314.2014.935298.

Möstl, C., et al. (2015), Strong coronal channelling and interplanetary evolution of a solar storm up to Earth and Mars, *Nat. Commun.*, *6*, 7135, doi:10.1038/ncomms8135.

Nakamura, M., A. Yoneda, M. Oda, and K. Tsubouchi (2015), Statistical analysis of extreme auroral electrojet indices, *Earth, Planets and Space*, *67*(1), 1–8. doi:10.1186/s40623-015-0321-0.

National Science and Technology Council (2015), National Space Weather Action Plan, Executive Office of the President of the United States, Washington D. C. [Available at https://www.whitehouse.gov/sites/default/files/microsites/ostp/final_nationalspaceweatheraction-plan_20151028.pdf, accessed 3 Mar 2016.]

Natural Resources Canada (2016), Magnetic Plotting Service. [Available at: http://www.spaceweather.gc.ca/plot-tracee/mp-en.php?plot_type=dbdt, accessed 2016-08-04.]

Ngwira, C. M., L.-A. McKinnell, and P. J. Cilliers (2011), Geomagnetic activity indicators for geomagnetically induced current studies in South Africa, *Adv. Space Res.*, *48*(3), 529–534.
Ngwira, C. M., A. Pulkkinen, M. Leila Mays, M. M. Kuznetsova, A. B. Galvin, K. Simunac, D. N. Baker, X. Li, Y. Zheng, and A. Glocer (2013), Simulation of the 23 July 2012 extreme space weather event: What if this extremely rare CME was Earth directed?, *Space Weather*, *11*, 671–679, doi:10.1002/2013SW000990.
Ngwira, C. M., A. A. Pulkkinen, E. Bernabeu, J. Eichner, A. Viljanen, and G. Crowley (2015), Characteristics of extreme geoelectric fields and their possible causes: Localized peak enhancements, *Geophys. Res. Lett.*, *42*, 6916–6921, doi:10.1002/2015GL065061.
North American Electric Reliability Corporation (2012), Effects of Geomagnetic Disturbances on the Bulk Power System., North American Electric Reliability Corporation, Atlanta, Ga. [Available at: https://www.frcc.com/Public%20Awareness/Lists/Announcements/Attachments/105/GMD%20Interim%20Report.pdf, accessed 2016-03-03.]
NRC (1990), Information Notice No. 90-42: Failure of Electrical Power Equipment Due to Solar Magnetic Disturbances. United States Nuclear Regulatory Commission. [Available at: http://www.nrc.gov/reading-rm/doc-collections/gen-comm/info-notices/1990/in90042.html, accessed 2016-03-22.]
OECD (2011), *Geomagnetic Storms*, Organisation for Econ. Co-operation and Dev., Paris.
Oughton, E., J. Copic, A. Skelton, V. Kesaite, Z. Y. Yeo, S. J. Ruffle, M. Tuveson, A. W. Coburn, and D. Ralph (2016), *Helios Solar Storm Scenario*, *Cambridge Risk Framework Ser.*, Cambridge Centre for Risk Studies, Cambridge.
Ouyang, M. (2014), Review on modeling and simulation of interdependent critical infrastructure systems, *Reliab. Eng. Syst. Saf.*, *121*, 43–60. doi:10.1016/j.ress.2013.06.040.
Pulkkinen, A., S. Lindahl, A. Viljanen, and R. Pirjola (2005), Geomagnetic storm of 29–31 October 2003: Geomagnetically induced currents and their relation to problems in the Swedish high-voltage power transmission system, *Space Weather*, *3*, S08C03, doi:10.1029/2004SW000123.
Pulkkinen, A., E. Bernabeu, J. Eichner, C. Beggan, and A. W. P. Thomson (2012), Generation of 100-year geomagnetically induced current scenarios, *Space Weather*, *10*, S04003, doi:10.1029/2011SW000750.
Pulkkinen, A., E. Bernabeu, J. Eichner, A. Viljanen, and C. Ngwira (2015), Regional-scale high-latitude extreme geoelectric fields pertaining to geomagnetically induced currents, *Earth Planets Space*, *67*(1), 93.
Rinaldi, S. M., J. P. Peerenboom, and T. K. Kelly (2001), Identifying, understanding, and analyzing critical infrastructure interdependencies, *IEEE Control Syst.*, *21*(6), 11–25, doi:10.1109/37.969131.
Rostoker, G. and T. Duc Phan (1986), Variation of auroral electrojet spatial location as a function of the level of magnetospheric activity, *J. Geophys. Res.*, *91*(A2), 1716–1722, doi:10.1029/JA091iA02p01716.
Samuelsson, O. (2013), *Geomagnetic Disturbances and Their Impact on Power Systems—Status Report 2013*, Lund Univ., Sweden.
Schrijver, C. J., R. Dobbins, W. Murtagh, and S. M. Petrinec (2014), Assessing the impact of space weather on the electric power grid based on insurance claims for industrial electrical equipment, *Space Weather*, *12*, 487–498, doi:10.1002/2014SW001066.
Schulte in den Bäumen, H., D. Moran, M. Lenzen, I. Cairns, and A. Steenge (2014), How severe space weather can disrupt global supply chains, *Nat. Hazards Earth Syst. Sci.*, *14*(10), 2749–2759, doi:10.5194/nhess-14-2749-2014.
Shiokawa, K., Y. Miyoshi, P. C. Brandt, D. S. Evans, H. U. Frey, J. Goldstein, and K. Yumoto (2013), Ground and satellite observations of low-latitude red auroras at the initial phase of magnetic storms, *J. Geophys. Res. Space Physics*, *118*, 256–270, doi:10.1029/2012JA018001.
Silverman, S. M. (2008), Low-latitude auroras: The great aurora of 4 February 1872, *J. Atmos. Sol. Terr. Phys.*, *70*(10), 1301–1308, doi:10.1016/j.jastp.2008.03.012.
Siscoe, G., N. U. Crooker, and C. R. Clauer (2006), *Dst* of the Carrington storm of 1859, *Adv. Space Res.*, *38*(2), 173–179.
Sonis, M., J. J. M. Guilhoto, G. J. D. Hewings, and E. B. Martins (1995), Linkages, key sectors, and structural change: Some new perspectives, *Dev. Econ.*, *33*(3), 243–246.
Space Studies Board (2008), Severe space weather events—Understanding societal and economic impacts: A workshop report [online], Natl. Academies Press, Washington, D. C. [Available at https://books.google.co.uk/books?hl=en&lr=&id=RLi3G4P7fIlC&oi=fnd&pg=PR1&dq=Severe+Space+Weather+Events+Understanding+Societal+and+Economic+Impacts::+A+Workshop+Report&ots=_cyJZNy5X9&sig=ivnVQiAxsXDN-f142VCzh8bsmXg, accessed 1 Jun 2015].
Sugiura, M. (1963), Hourly values for magnetic storm variation for International Geophysical Year. [Available at: http://ntrs.nasa.gov/search.jsp?R=19650020355, accessed 2016-03-23.]
Temmer, M., and N. V. Nitta (2015), Interplanetary Propagation Behavior of the Fast Coronal Mass Ejection on 23 July 2012, *Sol. Phys.*, *290*(3), 919–932. doi:10.1007/s11207-014-0642-3.
Thébault, E., et al. (2015), International Geomagnetic Reference Field: The 12th generation, *Earth, Planets and Space*, *67*(1), 1, doi:10.1186/s40623-015-0228-9.
Thomson, A. W. P., E. B. Dawson, and S. J. Reay (2011), Quantifying extreme behavior in geomagnetic activity, *Space Weather*, *9*, S10001, doi:10.1029/2011SW000696.
Timmer, M. P., E. Dietzenbacher, B. Los, R. Stehrer, and G. J. de Vries (2015), An Illustrated User Guide to the World Input–Output Database: The Case of Global Automotive Production, *Rev. Int. Econ.*, *23*(3), 575–605, doi:10.1111/roie.12178.
Torta, J. M., L. Serrano, J. R. Regué, A. M. Sánchez, and E. Roldán (2012), Geomagnetically induced currents in a power grid of northeastern Spain, *Space Weather*, *10*, S06002, doi:10.1029/2012SW000793.
Trivedi, N. B., et al. (2007), Geomagnetically induced currents in an electric power transmission system at low latitudes in Brazil: A case study, *Space Weather*, *5*, S04004, doi:10.1029/2006SW000282.
Tsurutani, B. T., W. D. Gonzalez, G. S. Lakhina, and S. Alex (2003), The extreme magnetic storm of 1–2 September 1859, *J. Geophys. Res.*, *108*(A7), 1268, doi:10.1029/2002JA009504.
Tsurutani, B. T., O. P. Verkhoglyadova, A. J. Mannucci, G. S. Lakhina, and J. D. Huba (2012), Extreme changes in the dayside ionosphere during a Carrington-type magnetic storm, *J. Space Weather Space Clim.*, *2*, A05, doi:10.1051/swsc/2012004.
Tsurutani, B. T., B. J. Falkowski, J. S. Pickett, O. Santolik and G. S. Lakhina (2015), Plasmaspheric hiss properties: Observations from Polar, *J. Geophys. Res. Space Physics*, *120*, 414–431, doi:10.1002/2014JA020518.
Tukker, A., and E. Dietzenbacher (2013), Global multiregional input–output frameworks: An introduction and outlook, *Econ. Syst. Res.*, *25*(1), 1–19.
U.S. Census Bureau (2010), Centers of Population. [Available at: https://www.census.gov/geo/reference/centersofpop.html, accessed 2016-08-04.]
U.S. Census Bureau (2014), Population Estimates. [Available at: http://www.census.gov/popest/data/historical/2010s/vintage_2014/state.html, accessed 2016-08-04.]
Watari, S. (2015), Estimation of geomagnetically induced currents based on the measurement data of a transformer in a Japanese power network and geoelectric field observations, *Earth Planets Space*, *67*(1), 1–12.

Watari, S., et al. (2009), Measurements of geomagnetically induced current in a power grid in Hokkaido, Japan, *Space Weather*, *7*, S03002, doi:10.1029/2008SW000417.

Wintoft, P., A. Viljanen, and M. Wik (2016), Extreme value analysis of the time derivative of the horizontal magnetic field and computed electric field, *Ann. Geophys.*, *34*(4), 485–491, doi:10.5194/angeo-34-485-2016.

World Input-Output Database (2016), WIOD Data. [Available at: http://www.wiod.org/new_site/database/wiots.htm, accessed 2016-08-05.]

Zhang, J. J., C. Wang, T. R. Sun, C. M. Liu, and K. R. Wang (2015), GIC due to storm sudden commencement in low-latitude high-voltage power network in China: Observation and simulation, *Space Weather*, *13*, doi:10.1002/2015SW001263.